Proceedings World Geothermal Congress 2020+1
Reykjavik, Iceland, April - October 2021

Geology, Exploration Wells Siting and Resource Estimation Using Power Density Method in Paka Geothermal Field

John Lagat and Geoffrey Mibei

Geothermal Development Company, P. O. Box 17700-20100, Nakuru, Kenya

jlagat@gdc.co.ke, gmibei@gdc.co.ke

Keywords: geology, exploration wells siting, resource capacity

ABSTRACT

This paper presents the results of a recent geological field survey, highlighting Paka eruptive history and structural geology. The findings are integrated to asses current exploration wells sites and give insights to Paka geothermal resource capacity. The new stratigraphic framework identifies seven (7) volcanic units comprising trachyte eruptions separated by basalt lava flows. The eruptive events in Paka were initiated in middle Pleistocene at 582 ka with climatic phase at 8 ka. The caldera formed between 70 ka and 35 ka, a much earlier period than proposed by previous researchers (11 ka). The area experienced intense tectonism between 278-205 ka during a period of hiatus in volcanism, creating most of the Paka localized faults as seen today. The faults are geothermally active and form interesting localities to target for exploration drilling. Structural considerations were employed during the siting and ranking of the 3 exploration wells sites PS-01 (PW-02), PS-02 (PW-01) and PS-03 (PW-03). Well site PS-02 was ranked higher compared to well site PS-01 and PS-03 because of fault intersection, soil gas anomaly and the fact that it is at the intersection between the caldera and the eastern crater. Well PW-01 was drilled to a depth of 2,553 m and discharged on test. The high potential anomalous area in Paka is about 20 km^2 based on structures, surface manifestations and soil gas anomalies. Resource assessment using the Power Density method indicates most likely (P50) a resource capacity of approximately 387 MWe. The optimistic (P10) high end of the range of power capacities is 640 MWe. It is worth noting that these estimations are based on limited surface and well data and as more geoscientific and wells data is acquired, and a 3-D numerical model is conducted, a more accurate estimate will be determined.

1. INTRODUCTION

Paka geothermal field lies between the inner tough of the Kenya rift (Figure 1). The system is hosted within a complex multi vent low basalt-trachyte volcano dominated by a young central caldera at the summit, which is 1.5 km in diameter and is slightly extended by the eastern and the western craters. The volcano is dotted with a number of smaller satellite volcanic centers, which are linked to the main volcano by linear zones of basalt and trachyte domes, tuff rings and eruptive fissures. The volcano rises 700 m above the rift floor to an elevation of 1697 masl.

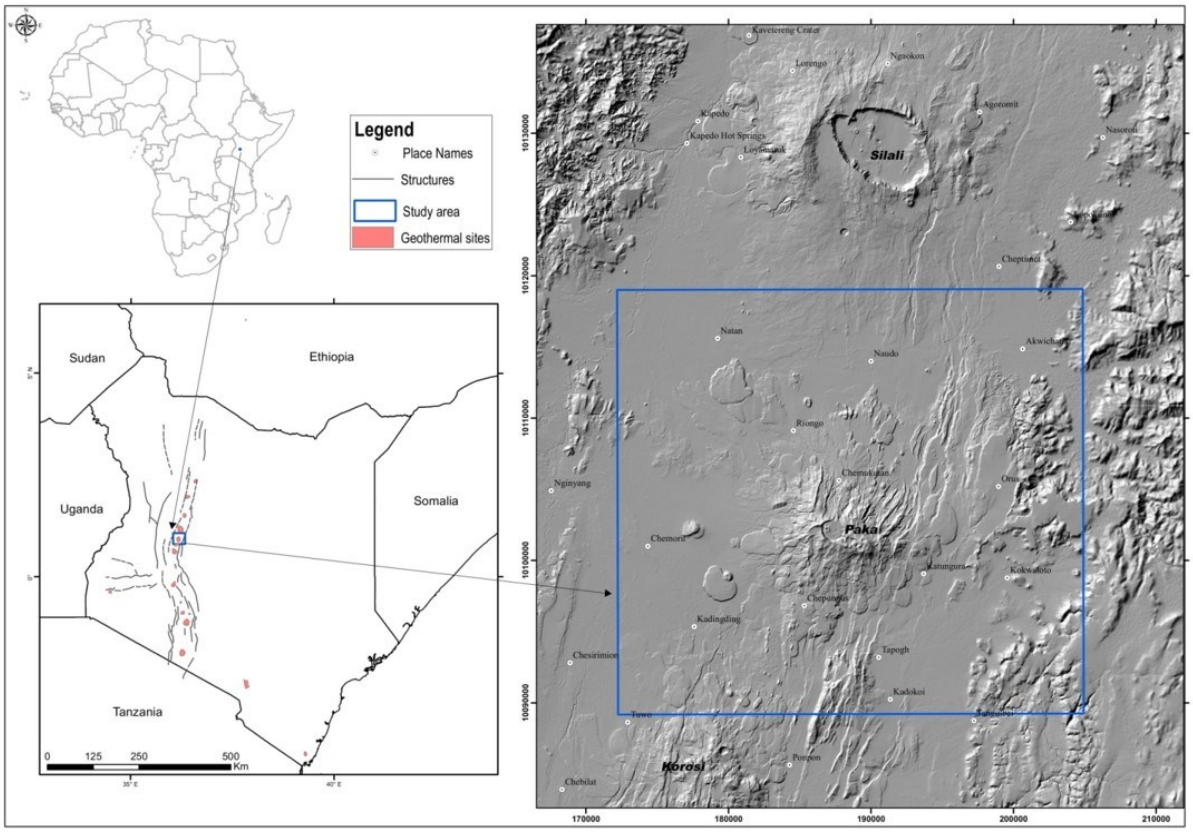

Figure 1: Map of the Kenya Rift showing the locations of major central volcanoes and the location of Paka geothermal field.

2. PREVIOUS WORK

Previous work in the area geared towards geothermal exploration includes geology, geochemistry and geophysics which concluded that there exists a geothermal system in Paka (Kanda et al., 2011). Geochemical survey results showed that non-condensable gas (NCG) content was low in the north of the caldera compared to intra caldera and eastern crater zone. This may be used as inference to the nature and quality of steam (Kipngok and Nyamongo, 2013) and demarcate zones of high heat influx or possible upflow zones. Gas geothermometry inferred reservoir temperatures of 250°C and a maximum temperature of 350°C. On the other hand, the resistivity structure implied an existence of a geothermal system with a resistive reservoir below the conductive layer. The conductive layer is presumed to be the system caprock, but the subject is enigmatic as the conductive layer is very thick and transgresses into the reservoir depths as proven by well PW-01.

3. METHODOLOGY

Field mapping survey was carried between June-August 2018 where field observations, data measures and samples were collected. A new surface geology map was generated by ArcGIS and based on constraints from available maps (Dunkley et al., 1993; Sceal, 1974; Williams, 1978), remotes sensing data and field observations. The remote sensing data used were the Google earth images and SRTM data of a 30 m resolution from Shuttle Radar Topography Mission (SRTM GL1, Source: https://doi.org/10.5069/G9445JDF). In addition, a review of available soil gas survey data, consisting of radon count measurements and carbon dioxide was done to further assess structural geology of Paka. Radon was collected using a RAD7 Durridge® alpha spectrometry instrument while the CO_2 percentage measurements were obtained by Orsat apparatus. Plots of geochemical data of log normal values versus cumulative probability were used in population discriminations (Chiodini et al., 1998) so as to generate data for classed spatial maps.

4. RESULTS

4.1 Surface Geology

Paka is a small shield volcano constructed largely by trachyte and basalt lavas and pyroclastic deposits. Basalt, hawaiite, mugearite, and lavas erupted from a series of fissure and fault zones located on the lower north western, northeastern and southern flanks. Volcanic activity commenced by 582 ka and continued until 8 ka. Contemporaneous trachytic and basaltic activity occurred in the main center and on a number of small satellites centers peripheral to the main volcanic edifice as show in the geological map (Figure 2). The oldest exposed rocks are the older trachyte and basalts, which constructed foundation for the volcanic shield. Subsequent faulting and fracturing of the shield by the NNE-trending and subordinate N-S faults occurred at 278-205 ka. Below is a description of each of the units in stratigraphic order.

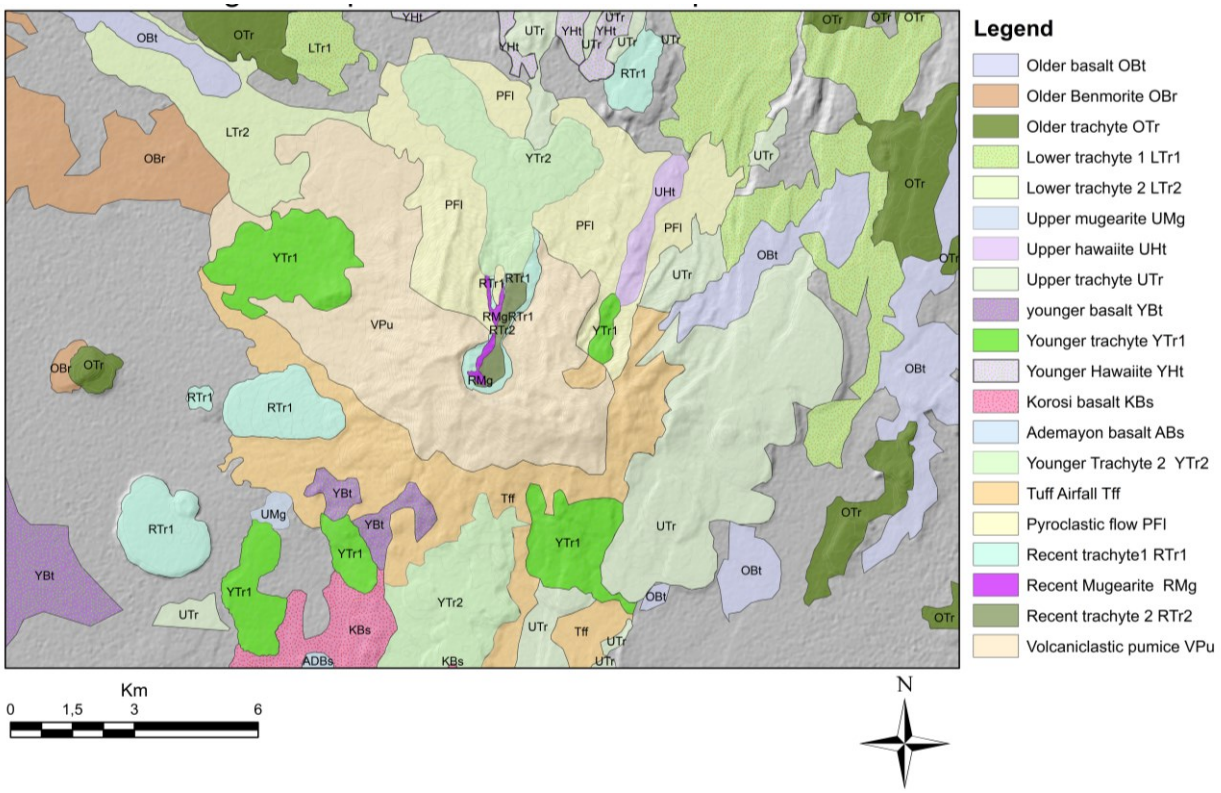

Figure 2: The geological map of Paka volcano and the surrounding (From present studies and Dunkley et, al., 1993).

4.1.1 Older Trachyte and Older Basalt

The oldest exposed rocks in the Paka geothermal field are the older trachyte, which constructed an early volcanic shield recognized by their eroded and faulted nature. The lava is exposed in a series of scattered outcrops peripheral to the lower flanks of the volcano in northwest and northeast. Petrographically the trachyte is fine grained with alkali feldspar phenocrysts up to 20 mm in length. The rock is also porphyritic with augite, and in some outcrops the rock is vesicular with the vesicles filled with pneumatolitic calcite and greenish clays. The lower trachyte is generally altered, and the rock is fissile and shows breaking along thin parallel sheets.

4.1.2 Lower Basalt and Lower Trachyte

The lower basalts are exposed in the lower plains to the southwest, southeast and on the eastern sides of Paka. The lower basalts are strongly faulted, eroded and thickly vegetated. Abundant spatter and scoria cones indicate that the most of the lower basalts were erupted from fissures. The formation is generally dark grey in colour and consists of up to 5 mm plagioclase feldspars, augite and olivine phenocrysts. The groundmass is made up of mainly tiny plagioclase laths. The rock formation is in most cases vesicular with the vesicles being infilled by pneumatolitic calcite and secondary clays. The formation is generally faulted and weathered.

4.1.3 Upper Trachyte and Upper Basalts

The upper trachyte is exposed on the southeast, on the western sector and on the northern plains of the volcano. The formation is vesicular to compact, fissile, fine grained and is porphyritic with alkali feldspars. The feldspar laths also show an aligned flow direction, a characteristic trachoid texture. Like the lower trachyte, the upper trachyte consists of alkali feldspars, pyroxenes, plagioclase, magnetite and to a small extent pyroxenes. To the northern plains, the formation is underlying the pyroclastic deposits that have buried the lava, exposing ribbon like outcrops marking flow fronts. The upper basalts occur on the northern and the southern plains and were erupted from NNE-trending fissures occurring both in the north and the south of the volcano. The matrix consists of feldspar, augite and magnetite crystals as euhedral laths in a granular groundmass. The rock is vesicular, with the small rounded vesicles occasionally being in-filled with secondary calcite. The rock has been affected by later faulting, forming a combination of horsts and grabens within the formation. The rock is generally less vegetated than the lower basalts. The upper basalts in the northeast host huge silica silnters deposits suggesting fossils hot spring in the area.

4.1.4 Younger Trachyte and Mugearite

Trachyte and mugearite are post caldera eruptions and are mainly erupted within the caldera flowing northwards. The trachyte has pronounced concentric ridges and multi lobate flow fronts up to 40 m high. The rock is fine grained and is porphyritic with feldspars, augite and tiny micro-phenocrysts of pyroxenes. The final stage of activity within the caldera was marked by the eruption of fluid mugearite from a scoria cone within the western half of the caldera. The lavas from this cone flowed southwards and eastwards across the trachyte on the caldera floor before flowing out of the breach and down on the northern flanks.

4.1.5 Pyroclastic and Volcaniclastic Deposits

The pyroclastic deposits form a large mantle averaging 30 m over the summit area and large parts of the western and the northern flanks of the volcano. The distribution was greatly affected by the prevailing easterly wind direction flow. The deposits were erupted from large trachyte and pumice cones on the summit area and from smaller cones aligned in a N-S direction on the summit area and the upper northeastern flanks. The pyroclastic is trachytic in composition and consists of pumice, obsidian and lithics of trachyte lava and large blocks of syenite. On the eastern crater, the pyroclastic is extensively altered to reddish and white (kaolinite and alunite) clays.

4.1.6 Recent Basalts

Occurrences of recent basalts were observed in the main caldera flow to the north. The recent basalts are less vegetated and still show the pristine flow morphology. The rock is fine grained to glassy and is vesicular at the edges and consists of phenocrysts of plagioclase, pyroxenes and tiny phenocrysts of augite.

4.2 Structural Geology

4.2.1 Faults and Fractures

Regional faults have previously been mapped in the area e.g. Dunkley et al. (1993), Sceal (1974), and Strecker and Bosworth (1991). In this survey, the younger faults referred to as the Paka axial faults are concentrated within axial zone and east of the caldera. They are akin to the Wonji faults in the main Ethiopian Rift mentioned e.g. in Abdulkadir and Eritro (2017), Agostini et al. (2011), Corti (2009) and Polun et al. (2018). Majority of the Paka faults are exposed east of the caldera, with few faults in the axial region due to masking effect of the younger volcanic products. Digital analysis of Paka faults using ArcGIS extraction tool and *Georose* software indicates that there is a variation in fault trends and that three populations are evident. A larger population of faults trend approximately N15°E, with subordinate populations trending N-S and approximately N26°E (Figure 3). Fractures mapped in the north, intra-caldera area and south of Paka caldera show a notable variation in the orientation including N-S, NW, NE and E-W. The N-S and E-W are the main trends displayed with N-S largely conforming to earlier regional stresses. The E-W component, however, differs from this regional trend and may be an indication of local scale accommodations zones that have been noted elsewhere in the rift (Dunkelman et al., 1989). Inferences from the crosscutting nature of the fractures indicate that the NW trending fractures are younger followed by the E-W, while the N-S are the oldest.

4.2.2 Eruption Centers or Volcanic Vents

Lava flows from Paka were either erupted from fissures or eruption centers/volcanic vents. Eruption centers are numerous in Paka and during the field work an attempt was made to analyze the orientation of how their outline and rims of the craters were elongated using DEM images and ARGis platform. Results show that the orientation of the eruption centers in Paka largely conforms to the N-S regional fault trends. This infers a linkage between tectonic and magmatism and may suggest larger interplay between structures, magma conduit and diking system.

4.2.3 Fissures, Inferred Faults and Lineaments

Fissures were identified as open linear features with no visible displacement and appeared to have been associated with lava eruptions. They are indicated by the red lines in the structural map (Figure 3). The fissures were dominant in the north and minor in the south of the Paka caldera. They appear to have played a significant role in controlling fissure eruptions from initial development of Paka where diffuse eruption was initiated east of Paka caldera. Lineaments and inferred faults were mapped in the south and north of the caldera. They display a general trend of N-S, N-W and E-W. The E-W could further confirm the presence of E-W accommodation

zones as suggested earlier from mapped fractures. The N-S trends conform to a regional fault trend while the N-W agrees with fracture trends.

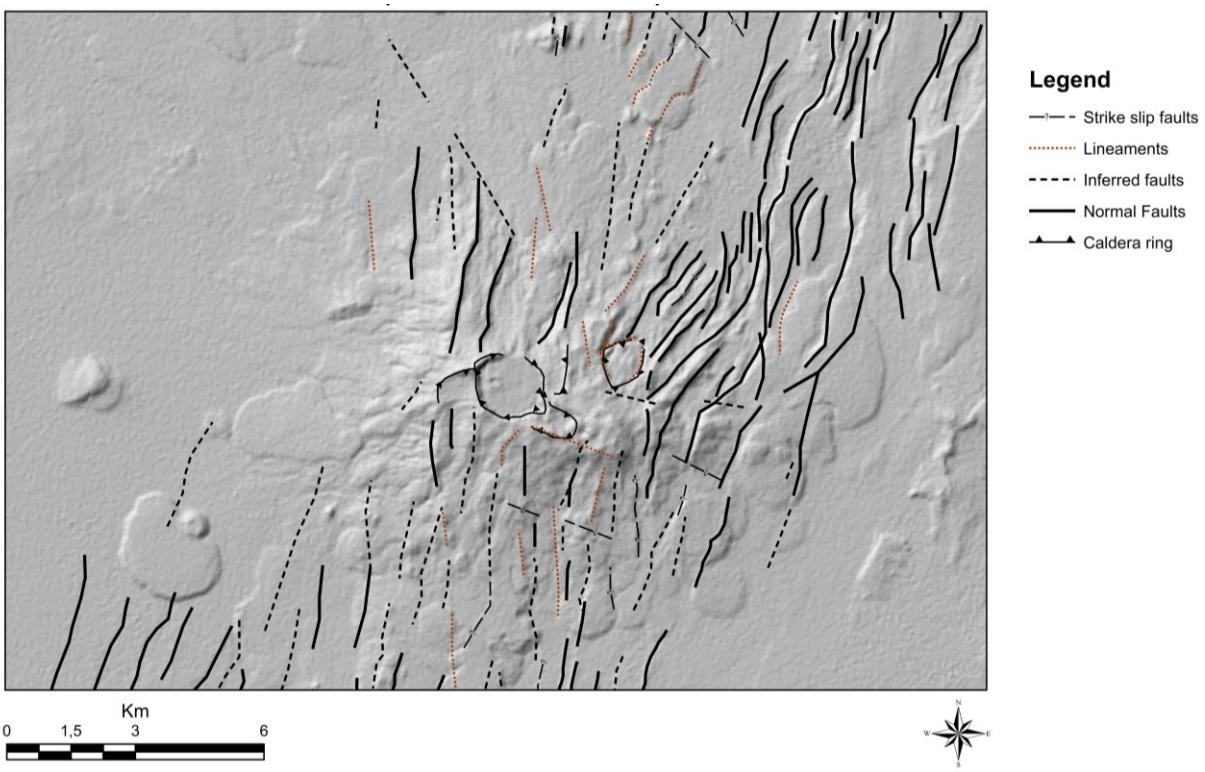

Figure 3: Updated structural map of Paka geothermal field.

4.3 Structural and Hydrothermal Inferences from Soil Gas Data

Soil gas data from previous surveys were reassessed with the purpose of mapping out buried structures and constraining the possible geothermal area. This involved the analysis of radon and CO_2 gas data. Radon is a radiogenic gas from uranium and thorium radioactivity. These parent elements are rare earth (REE) elements and are incompatible during most of the magmatic process and are therefore enriched in crustal rocks.

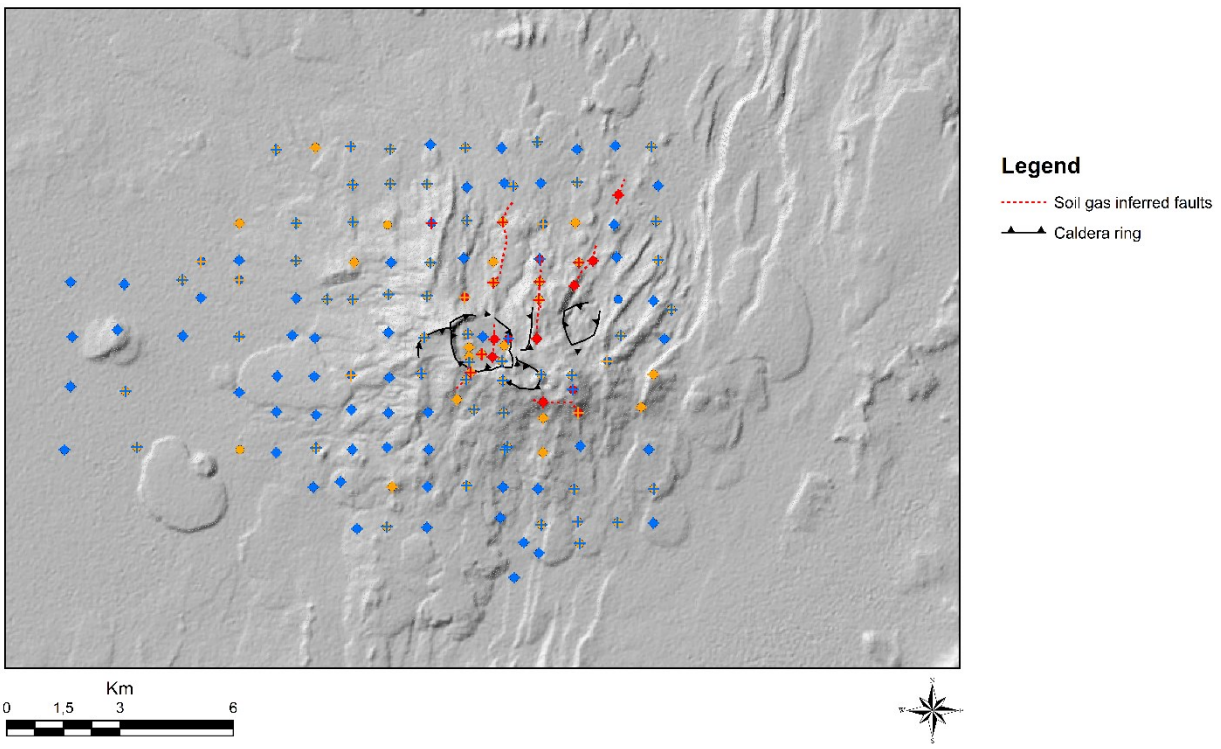

Figure 4: Inferred soil gas structures in Paka Geothermal field.

Radon-22, which is of interest in this survey, has a half-life of 5 second and therefore, for it to be detected on surface it must have degassed rapidly from the source. For this to occur the assumption is that there are pathways or permeability which could be related to faults, fracture etc. The anomalous levels of radon gas (Rn-222) is therefore used to infer geological structures. CO_2 on the other hand is a magmatic gas but can also be biogenic. However, in geothermal areas such as Paka, we assume that most of the CO_2 gas is magmatic, insoluble and partitions favorably to the steam fraction of hot areas. This can be picked from soil gas as anomalies in high temperate localities associated with hydrothermal fluid flow linked to pathways or geological structures. The exploratory data analysis or EDA was used to discriminate population which were plotted on a map view. Three populations were discriminated for radon and CO_2 which was plotted in a map view highlighted in Figure 4. The results indicate linear relations, showing possible structures in north east and south east of Paka with N-S, N-W and E-W trends.

5. DISCUSSIONS AND CONCLUSIONS

5.1 Paka Updated Structural Map

The updated structural map (Figure 5) is based on previous surveys and current data. The new additions are the N-E and E-W trending structures from soil gas and field observations. Of particular interest are the E-W, suggesting that Paka main center is within a structural intersection zone and explain why lava eruptives were concentrated there. This zone is a hydrothermal anomalous zone with manifestations occurring in the area, which from a volcanological point of view is a point source for the recent lava eruptions. Generally, the east and northwest of Paka appear to have been under huge volcanic influences being the highest point topographically. In this area fumaroles and collapse structures occur. The fossil hot springs in the northeast suggest an outflow zone, which would be facilitated by the structures as the structural trend suggests.

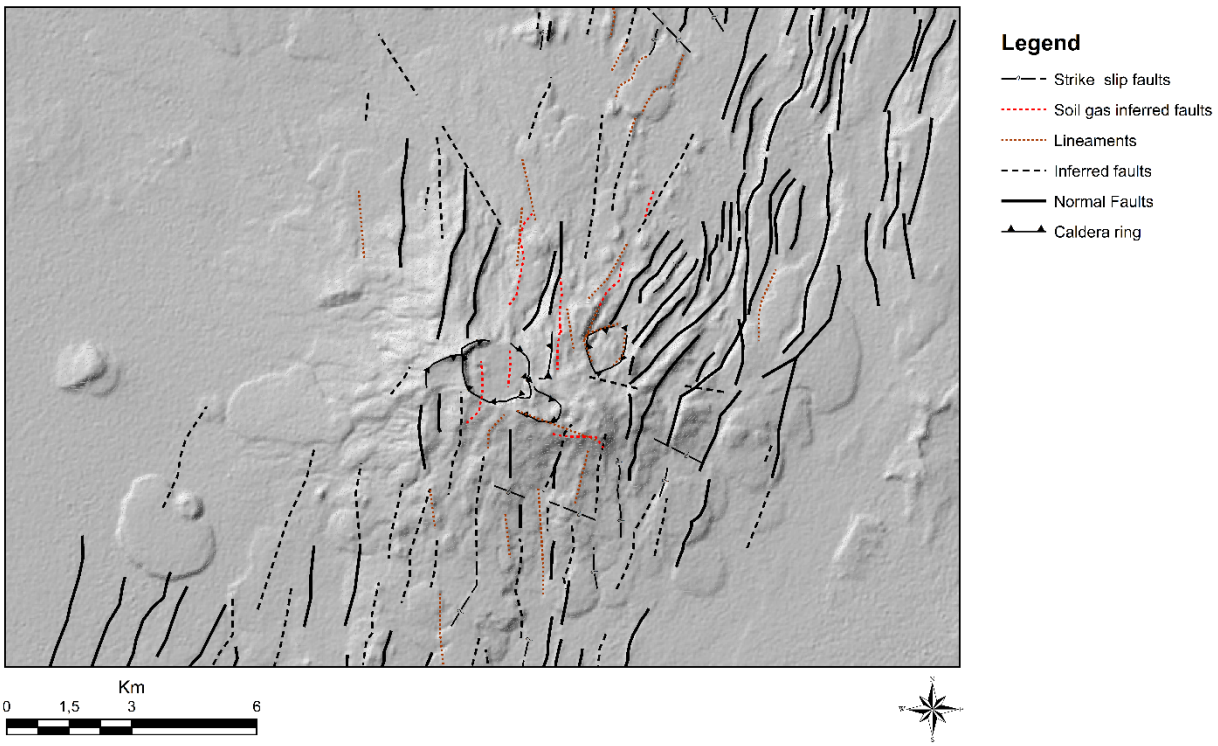

Figure 5: Updated structural map of Paka geothermal field.

5.2 Resource Area and Assessments of Geothermal Exploration Well Sites in Paka

Integrated structural data from field observation, remote sensing and soil gas data together with surface manifestations constrains an area of around 20 km^2 (Figure 6). There are three exploration wells sited in Paka (Figure 6) and well PW-01 has already been drilled to a depth of 2,523 m and discharged on test. Generally, the three sites were sited based on structural association and hydrothermal manifestations. Here, the available data was examined closely in order to rank the wells sites. Site PS-02 (well PW-01) was sited east of the main Paka caldera. It is within the caldera ring fault and an intersection of faults, and there is a mild soil gas anomaly near the well. The faults, fault intersection and soil gas anomaly make the well a site to be highly ranked. The well has since discharged on test. Site PS-01 (well PW-02) was sited north of the caldera and is generally within the inferred structural zone and in a hydrothermally active zone based on soil gas data. The convergence of structural and hydrothermal active zones makes this site ranked as second. The well is currently being drilled. Site PS-03 (well PW-03) is sited within the inferred fault intersection area and caldera rim edge and the western cater. No soil gas anomaly was however encountered in the site properly due to the thick pyroclastic cover because of the prevailing westerly winds. This well is therefore ranked third and will be drilled after completion of well PW-02.

5.3 Resources Assessment

5.3.1 The Heat Source

Eruptions in Paka occurred continuously for over 500 ka, i.e. 582 ka to 8 ka. Paka volcano is made predominantly of trachytic volcanism with minor basaltic lavas erupted within the caldera and in the flanks along the NNE-SSW trending fissures. The magma chamber in Paka is still active as indicated by the eruptions of the Holocene basalt lavas within the caldera and along fissures to the north of the volcano. Occurrences of shallow intrusives are evidenced by the presence of abundant syenitic nodules within the

pyroclastic deposits that were erupted during the formation of the caldera at Paka and from the recovered well cuttings from well PW-01. The main heat source for the geothermal system at Paka is therefore shallow trachyte or trachyte-basalt intrusives or intrusion complexes, within the volcano. These bodies are long lived and have been kept alive by re-injection from time to time of fresh pulses of magma from depth. Presence of well-crystallized sulphur deposits at fumaroles found at the eastern crater indicates that the faults are deep seated and are magmatic derived.

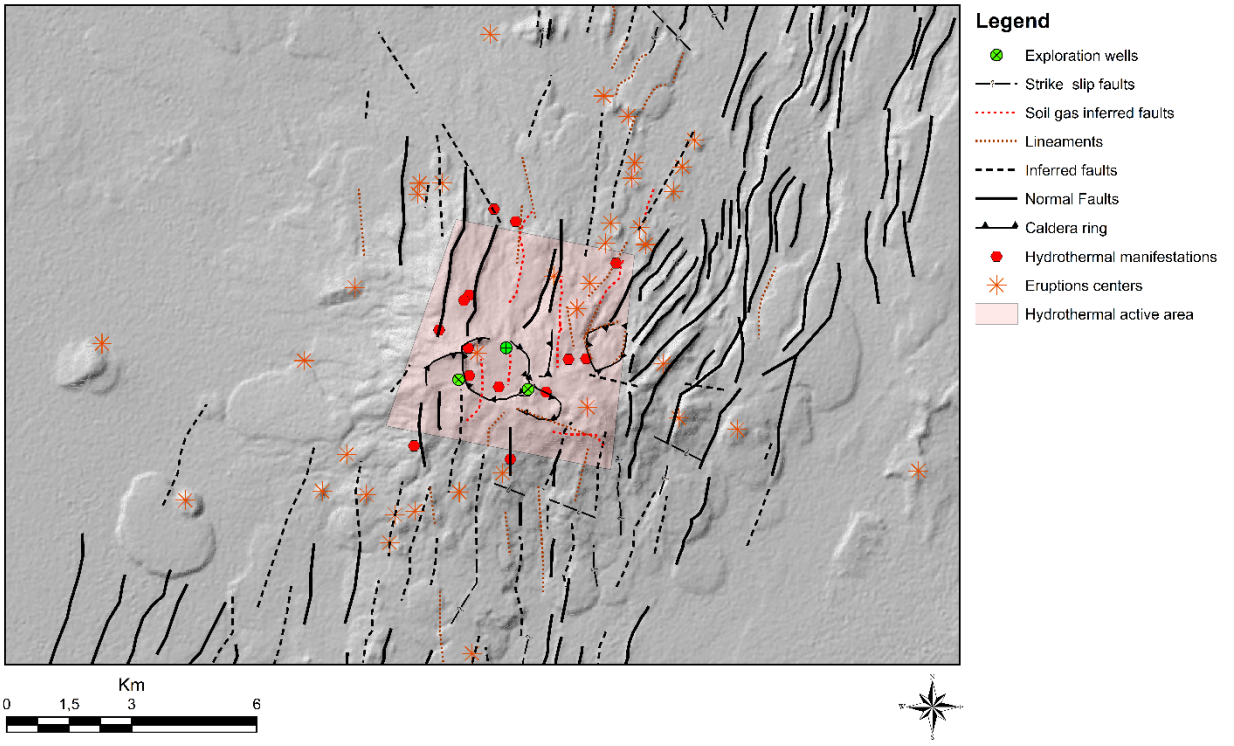

Figure 6: Paka resource area, manifestations, faults, soil gas anomalies and wells sites.

5.3.2 Recharge

Ground water flow in the North Rift area around Paka is presumed to be a combination of the lateral flow from the rift margin and the northerly axial flow along the inner trough of the rift floor. The recharge is laterally from the Laikipia Escarpment in the east and Baringo range in the west and axially, Lake Baringo in the south is probably recharging the prospect as indicted by the general northern groundwater flow along the rift floor. Meteoric water from the wetter and higher rift margins are channeled to the rift floor though the major rift flank faults and are directed and modified within the rift floor by the rift floor fault network and dykes, which allow for water to follow longer deeper paths to the heat sources.

5.3.3 Permeability

Strong surface manifestations in the Paka prospect indicate presence of a complete hydrothermal system whereby there is recharge, permeability, heat source and return path to the surface. Local N-W regional structures and the NNE-NNS and N-S trending faults and fractures are essential in enhancing permeability in the prospect area. Logs from well PW-01 and shallow borehole data indicate that additional aquifers were mainly encountered on fractured volcanics, volcaniclastic sediments and at lithological contacts.

5.3.4 Reservoir and System Capping

The reservoir rocks are trachyte and basalts with, minor intercalations of tuff and syenites at the bottom as suggested by the results of well PW-01. The geothermal resource has been proven by the discharging well PW-01 and reservoir thickness is estimated to be 1200-1400 m. The system's cap is still enigmatic however, it is envisaged to be the trachyte and basalt lavas and their associated pyroclastics, which provide for proper sealing to confine the geothermal fluids.

5.3.5 Resource Capacity from Power Density Estimation

Resource capacity estimates are commonly made using power density, natural heat loss, stored heat, and numerical modeling (Benoit, 2013; Grant and Bixley, 2011). The most robust resource capacity estimates are made using a 3-D numerical model of the reservoir, coupled to well bore models of the production and injection wells, and informed by extensive and detailed geoscientific data. However, in the exploration and development stages of a geothermal project, and even into the early production phase, these data and models may not be available. Inevitably, power density is normally invoked for first-order estimates of resource capacity, usually expressed in terms of MW/km^2. The benefit of using power density is that it instantly returns a reasonable value, while stored heat estimates may be in error by orders of magnitude (Cummins, W, B., 2016) and numerical models require significant time and effort to build but may not be any more accurate than the power density unless they are well calibrated.

Table 1: Reservoir parameters.

Parameter	Min	Best value	Max	Comments
Area (km^2)	20	25	30	Area constrained by manifestations, caldera eruption centers and active faults
Thickness (m)	1000	N/A	1600	Based on geology logs of well PW-01
Reservoir temperature (°C)	200	250	320	Based on gas geothermometry

The selected range of power densities was based on the plot of Power Density versus Average Reservoir Temperature for 80 operating fields (Figure 7). The geology at Paka prospect is described as faulted and volcanic in nature. The tectonic setting is interpreted to be mainly volcanic. The estimated reservoir temperature of 250°C was determined from gas geothermometry, therefore, a reservoir temperature range of 250-300°C was chosen. The apparent high permeability encountered due to high Radon-222 measurements justifies using a larger power density range than indicated by the main sequence plot line. The reservoir temperature range and the tectonic setting deduced for Paka geothermal prospect corresponds to an expected power density range of 10-25 MW/km^2 (Figure 7).

The power density method assigns exploration confidence factors for the probability of discovering commercial temperature, permeability and probable reservoir chemistry (Figure 8). Given the inferred temperatures of approximately 250°C, the confidence index of 90% for the reservoir temperature was chosen. Similarly, a higher confidence index of 90% was chosen for the permeability within the Paka geothermal area based on the soil gas chemistry which determined Radon-222 anomaly indicative of high permeability. A high probability of 99% was chosen for reservoir chemistry since it is not a factor during exploration stage of geothermal development. The combination of these factors results in a probability of exploration success (the probability that at least one commercial well will exist) of 80%.

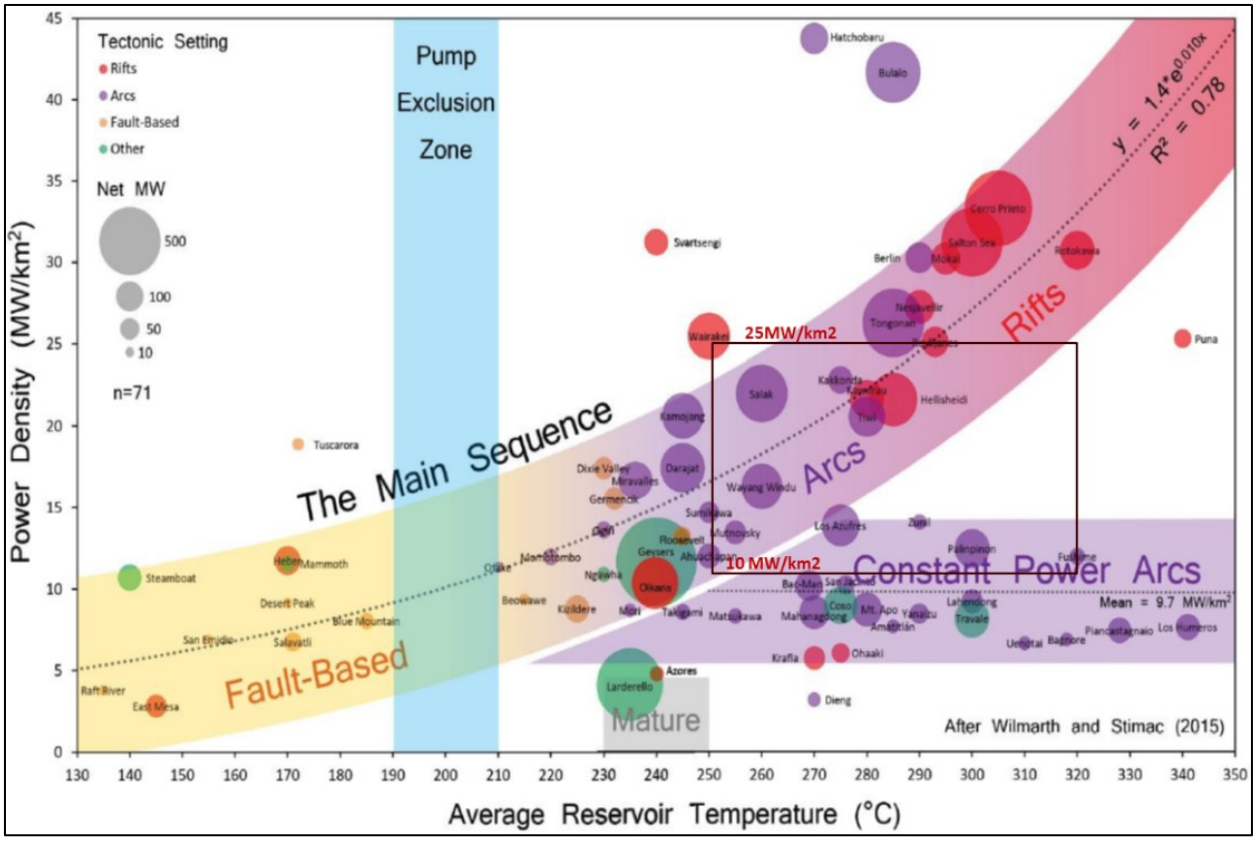

Figure 7: Power density versus reservoir temperature categorised by geological setting (Wilmarth et al., 2015) indicating power density range of 10-25 MW/km^2 for the prospect given reservoir temperature range of 250-320°C in a volcanic arc tectonic setting.

The results (Figure 8 and 9) indicate that an expected field development resource capacity of about 387 MWe is possible. The optimistic (P10) high end of the range of power capacities is 640 MWe. These estimations are of course preliminary and as more geoscientific and well data is acquired and a reservoir feasibility study using 3-D numerical simulation model is carried out, a more accurate estimate will be determined.

Geothermal Power Capacity Reserve Estimation: based on Lognormal Distributions of Area and Power Density

EXLORATION: Is it there?

Assuming a likely exploration geoscience program and drilling program, what is the percent confidence that at least one well is commercial

	Confidence in temperature.		Confidence in permeability. Commercial mDarcy		Confidence in chemistry. Not corrosive or scaling		Probability of exploration success
	PTemperature		**PPermeability**		**Pchemistry**		**POSexpl**
Exploration Confidence	0.90	*	0.90	*	0.99	=	0.80

APPRAISAL AND DEVELOPMENT: Assuming it's there, how big is it?

Cumulative confidence of representative optimistic case = **10%** That is, the larger, more optimistic case is assumed to be P10

Temperature range of permeable reservoir area from resource conceptual model. This should be consistent with assumed power density distribution.

Startup average production temperature for P90 reserves = **320** °C **250** °C = minimum temperature for P10 reservoir

Nu and Sigma are the mean and variance in log units required for specifying lognormal distributions in tools like @RISK

Representative Cases		P99	P90	Pessimistic P90	Middle P50	Optimistic P10	P10	P01	Mean	nu	sigma
Area > 250°C	**(km^2)**	17.0	20.0	**20.0**	24.5	**30.0**	30.0	35.4	24.8	3.19846	0.15819
Power Density 250 to 320 °C	**(MWe/km^2)**	7	10	**10.0**	16	**25.0**	25	36	17	2.76073	0.35749
MWe Capacity		156	235	234.7	**387**	639.2	639	962	418	5.95920	0.39093

EXPECTED POWER CAPACITY RESERVES (based on analogous reservoirs used to assess confidence in power density and area)

Expected Mean Capacity = 335 MWe = [Probability of Exploration Success] * [Mean Capacity of Development Assuming Exploration Success]

Expected P50 Capacity= 310 MWe = [Probability of Exploration Success] * [P50 Capacity of Development Assuming Exploration Success]

Adapted from Cumming, W., 2000. Spreadsheet for geothermal resource capacity scoping using lognormal area and power density distributions. Proprietary course material.

Figure 8: Paka reservoir Potential Power Capacity reserve calculation based on lognormal distributions of Area and Power Density (After Cumming 2016). The expected mean capacity is 335 MWe and the P50 (most likely) capacity is 387 MWe.

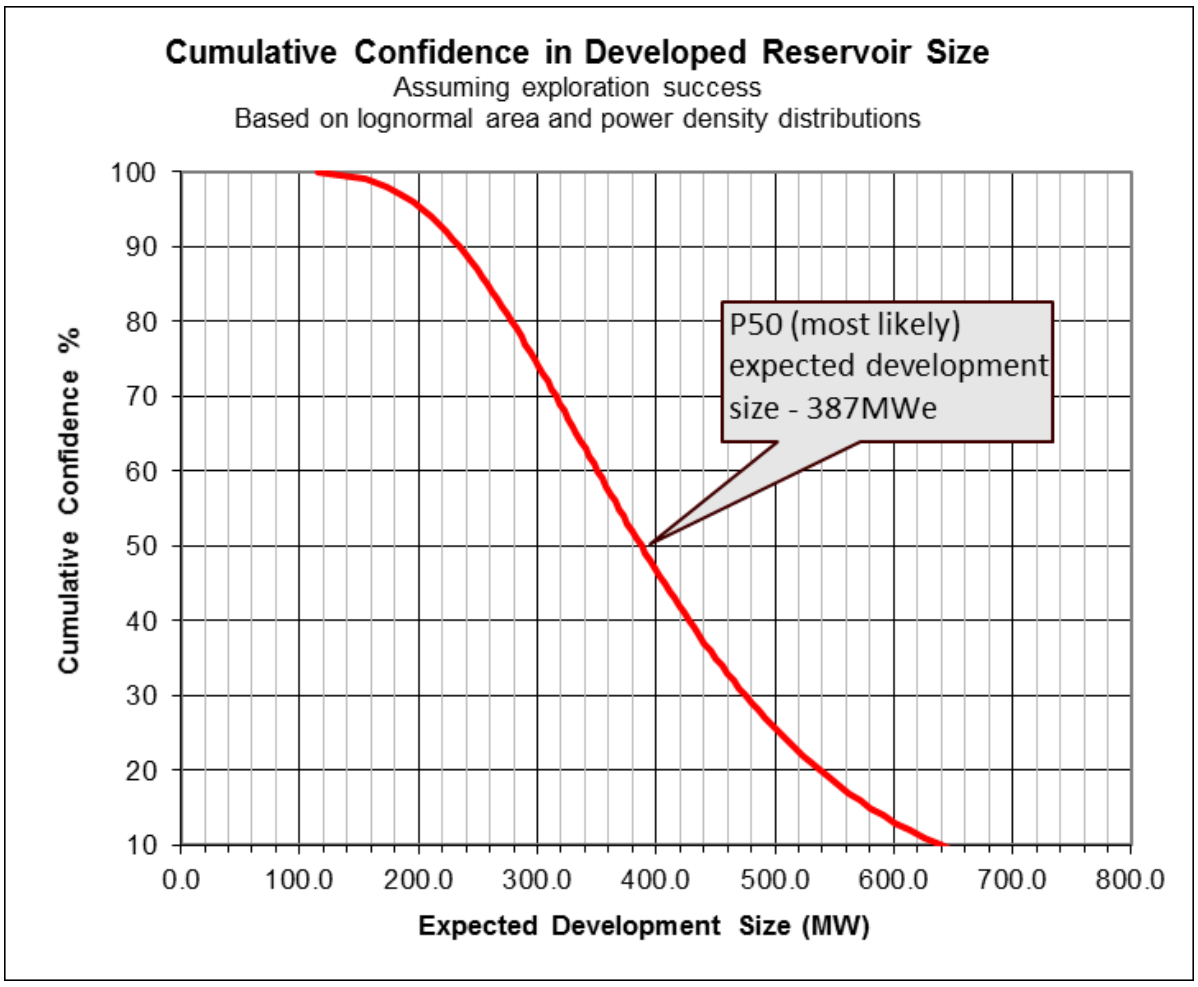

Figure 9: Expected development size of Paka reservoir capacity P50 (most likely) capacity is 387 MW and an optimistic P10 reservoir capacity is 640 MWe.

REFERENCES

Abdulkadir, Y. A., Eritro, T. H. (2017). 2D resistivity imaging and magnetic survey for characterization of thermal springs: A case study of Gergedi thermal springs in the northwest of Wonji, Main Ethiopian Rift, Ethiopia. *Journal of African Earth Sciences, 133*, 95-103. doi: https://doi.org/10.1016/j.jafrearsci.2017.05.001

Agostini, A., Bonini, M., Corti, G., Sani, F., Mazzarini, F. (2011). Fault architecture in the Main Ethiopian Rift and comparison with experimental models: Implications for rift evolution and Nubia–Somalia kinematics. *Earth and Planetary Science Letters, 301*(3), 479-492. doi: https://doi.org/10.1016/j.epsl.2010.11.024

Benoit, D.: An Empirical Injection Limitation in Fault-Hosted Basin and Range Geothermal Systems, *Geothermal Resource Council Transactions*, 37, (2013), 887-894.

Chiodini, G., Cioni, R., Guidi, M., Raco, B., Marini, L. (1998). Soil CO_2 flux measurements in volcanic and geothermal areas. *Applied Geochemistry, 13*(5), 543-552. doi: https://doi.org/10.1016/S0883-2927(97)00076-0

Corti, G. (2009). Continental rift evolution: From rift initiation to incipient break-up in the Main Ethiopian Rift, East Africa. *Earth-Science Reviews, 96*(1), 1-53. doi: https://doi.org/10.1016/j.earscirev.2009.06.005

Cummins., W, B., 2016: Geothermal Resource Capacity Estimation Using Lognormal Power Density from Producing Fields and Area from Resource Conceptual Models; Advantages, Pitfalls and Remedies

Dunkelman, T. J., Rosendahl, B. R., Karson, J. A. (1989). Structure and stratigraphy of the Turkana rift from seismic reflection data. *Journal of African Earth Sciences (and the Middle East), 8*(2), 489-510. doi: https://doi.org/10.1016/S0899-5362(89)80041-7

Dunkley, P., Smith, M., Allen, D. J., Darling, W. G. (1993). The geothermal activity and geology of the northern sector of the Kenya Rift Valley (Vol. SC/93/1).

Germinario, L., Siegesmund, S., Maritan, L., Mazzoli, C. J. E. E. S. (2017). Petrophysical and mechanical properties of Euganean trachyte and implications for dimension stone decay and durability performance. *76*(21), 739. doi: 10.1007/s12665-017-7034-6

Grant, M. A., and Bixley, P.F.: Geothermal Reservoir Engineering 2nd Edition, Elsevier, Amsterdam, (2011), 359.

Kanda, I., et al., 2011: Paka geothermal prospect, investigations for its geothermal, potential. A Geothermal resource assessment project report. GDC Internal Report

Kipngok, J., Nyamongo, J. (2013). Fumarole Gas Geochemistry of Paka Geothermal Prospect, North Rift, Kenya. *GRC Transactions, Vol. 37*. doi:

Polun, S. G., Gomez, F., Tesfaye, S. (2018). Scaling properties of normal faults in the central Afar, Ethiopia and Djibouti: Implications for strain partitioning during the final stages of continental breakup. *Journal of Structural Geology, 115*, 178-189. doi: https://doi.org/10.1016/j.jsg.2018.07.018

Sceal, J. S. C. (1974). The Geology of Paka Volcano and the Country to the East, Baringo District, Kenya: University of London.

Strecker, M., Bosworth, W. (1991). Quaternary stress-field change in the Gregory Rift, Kenya (Vol. 72).

Williams, L. A. J. (1978). Character of Quaternary volcanism in the Gregory Rift Valley. *6*(1), 55-69. doi: 10.1144/GSL.SP.1978.006.01.06 %J Geological Society, London, Special Publications.

Wilmarth, M., Stimac, J (2015). Power density in geothermal fields. *Proceedings World Geothermal Congress 2015, Melbourne, Australia*